ALICE/94-29
Internal Note/EMC
9 November 1994

FURTHER PROGRESS IN LEAD TUNGSTATE CRYSTALS

A. Fyodorov[1], M. Korzhik[1], O. Missevitch[1], V. Pavlenko[1],
V. Kachanov[2], A. Singovsky[2], A.N. Annenkov[3], V.A. Ligun[3],
J.P. Peigneux[4], J.P. Vialle[4], J.L. Faure[5], F. Binon[6].

ALICE Seminar of 11th November 1994

[1] INP, Minsk, Belarus
[2] IHEP, Protvino, Russia
[3] Spectr Co. Research Div., Tula, Russia
[4] LAPP, Annecy, France
[5] DAPNIA, CEA, Saclay, France
[6] IISN, Brussels, Belgium.

Further Progress in Lead Tungstate Crystals

A. Fyodorov, M. Korzhik, O. Missevitch and V. Pavlenko, INP, Minsk, Belarus
V. Kachanov and A. Singovsky, IHEP, Protvino, Russia
A.N. Annenkov and V.A. Ligun, Spectr Co, Research Div., Tula, Russia
J.P. Peigneux and J.P. Vialle, LAPP, Annecy, France
J.L. Faure, DAPNIA, CEA, Saclay, France
F. Binon, IISN Brussels, Belgium

I. Introduction

Recently, lead tungstate $PbWO_4$, also called PWO crystals, have been considered as a promising material for precise electromagnetic calorimetry [1–7] and the first tests have shown that energy resolution, with photomultiplier readout, better than $3\%/\sqrt{E} \oplus 0.7$ can already be achieved with a calorimeter prototype of 9 or 20 counter cells ($20 \times 20 \times 180 + 200$ cm^3). Among the relevant properties of the crystal, its good radiation hardness has been specially mentioned as well as its short radiation length and its emission in the blue range of the spectrum. Further development in PWO technology to improve the transparency and uniformity of long crystals suitable for calorimetry has been undertaken. The usual growing conditions for normal $PbWO_4$ crystals have been tuned for a better control of stoichiometry, and investigation of pentavalent doping has been explored.

II. Spectroscopic and Scintillation Properties of PWO Scintillators

A. *Transparency and Growing Conditions*

The improvement of PWO scintillation properties depends on the minimization of defects in the crystals based on Pb^{3+} ions, caused by a shortage of cation in the W position [8]. As a result the transmission spectrum measured through a 20 mm thickness transversally to the growing axis of test crystal cells presents a difference between the seed side (also called top side) and the other extremity of the crystal (also called bottom side). This difference is shown on Fig. 1(a) for crystal grown in a limited-volume crucible of 100 mm in diameter.

A better uniformity of transmission along the crystal has been obtained by using a larger diameter crucible (120 mm) and using increased atmospheric pressure in the growing chamber. This is shown on Fig. 1(b) where no transmission spectrum difference has been observed between the top part and the bottom part of the crystal.

To minimize as much as possible the appearance of Pb^{3+} defects or others, doping by Nb has also been used and found satisfactory [8]. Improvement of transparency along the Nb-doped crystal has been obtained as shown on Fig. 1(c). Compared with the crystal grown with the stoichiometry stabilization of Fig. 1(b), transparency in the 300–400 nm wavelength range has been significantly improved. Nevertheless, a weak absorption band appears near 420 nm.

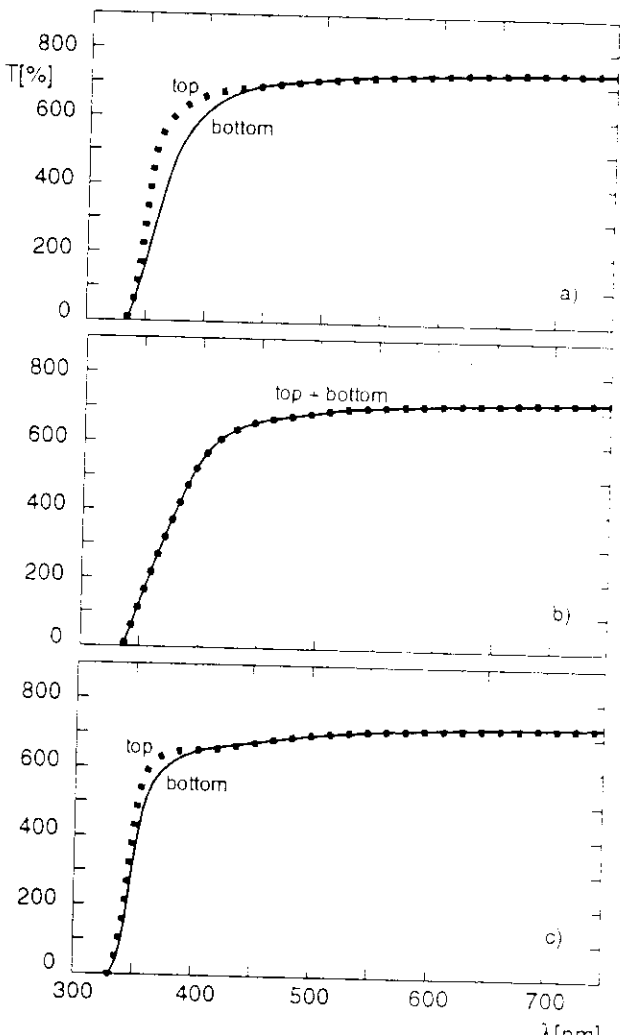

Fig. 1 Transmission curve through a 20 mm thickness of PWO crystal – top and bottom: a) grown in 100 mm diameter crucible; b) grown in 120 mm diameter crucible under increased atmospheric pressure in the chamber; c) grown with optimal Nb doping content.

B. Luminescence of Nb-Doped Crystal

To study the Nb doping effect on PWO crystal properties, a set of crystals containing different amounts of Nb has been investigated. All full-size crystals (with a length of at least 220 mm) were grown from the same crucible in the same conditions. The first crystal was grown without doping. For the other ones the Nb content expressed as a percentage of melt mass were 0.001 (N2), 0.0036 (N3), 0.0079 (N4), 0.015 (N5), 0.019 (N6), 0.022 (N7). The reference samples for detailed investigations with dimensions $10 \times 10 \times 10$ or $20 \times 20 \times 10$ mm^3 were cut from the top of the grown ingot; for the N3 and N6 samples, pieces were also cut from the top and the bottom of the crystal. The distance between the top and the bottom samples cut from the same ingot is at least 190 mm.

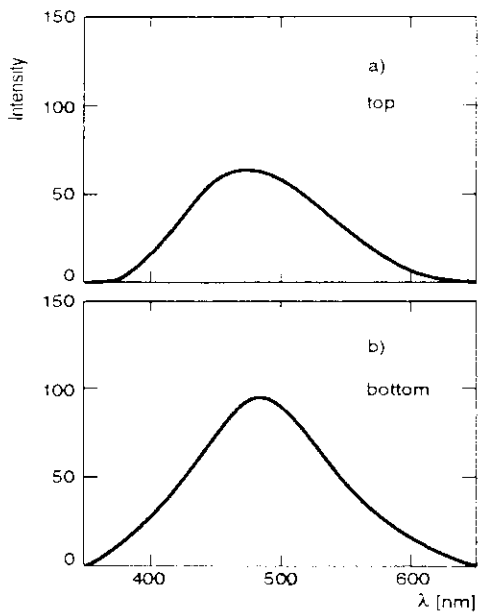

Fig. 2 γ-ray (^{57}Co, 122 KeV) excited luminescence of the PWO:Nb samples N3, extracted from the top (a) and bottom (b) of the crystal. T = 300 K.

The luminescence spectra excited by γ-rays are practically the same for the top and the bottom part of the crystal doped with a small amount of Nb. The luminescence spectra for the N3 sample are presented in Fig. 2 for the top and bottom parts. Although the Nb ions change the balance of the radiating centres in the crystal, the overall luminescence spectrum shape is not affected by the increasing proportion of $(NbO_3 + F^+)$ centres at the bottom part of the crystal.

III. Decay Time and Light Yield of Nb-Doped Crystal

A. Decay Time Measurement

The scintillation kinetics for Nb-doped PWO crystal samples has been measured by the usual start-stop method. Their decay time curves are well fitted by two exponential functions approximation.

$$A1 \times \exp(-t/\tau_1) + A2 \times \exp(-t/\tau_2) + A3$$

where A3 is the noise level of random coincidences.

The main parameters τ_1 and τ_2 of the fit are presented in Fig. 3 where N1 refers to the undoped crystal of the grown set. The slight decrease of τ_1 and especially of τ_2 with sample number is attributed to the domination of the $(NbO_3 + F^+)$ centres' amount on the green luminescence $(WO_3 + F)$ centres' amount with the increase of the Nb content in the melt. So the scintillation of crystals with a significant amount of Nb ions is mainly produced by WO_3^{2-} centres and $(NbO_3 + F^+)$ centres with decay time constants 2.5 ns and 12 ns, respectively.

The difference between the kinetics of the top and bottom samples is small. The observed variation of decay time constants with increasing Nb content seems in good agreement with the scintillation mechanism expected from the model proposed elsewhere [8].

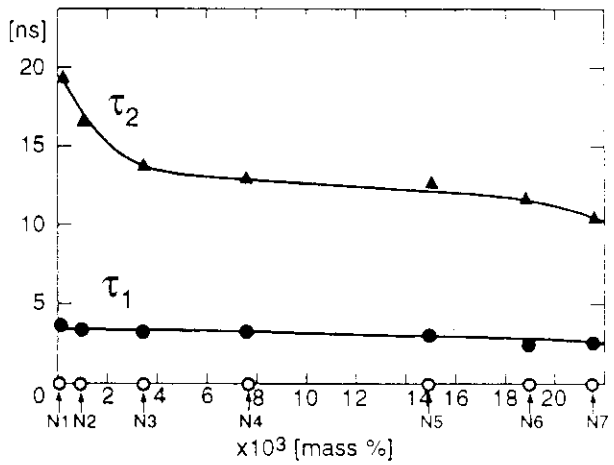

Fig. 3 Decay time constant variation of Nb-doped sample ($10 \times 10 \times 10$ cm^3) versus Nb content in the melt during crystal growth.

B. Light Yield

The evaluation of light yield in photoelectrons/MeV has been obtained by comparison of the photopeak position of the 1.2 MeV γ-rays of ^{60}Co source measured by a Philips 2262 photomultiplier and the single electron peak of the phototube. These measurements have been done for reference samples as well as for 180 mm full-length crystals. For reference sample N3 (bottom part) 40 photoelectrons/MeV have been estimated. The effect of the Nb content in the reference samples on their light yield is summarized in Fig. 4 where the different samples are indicated on the horizontal scale referring to Nb content in mass per cent. Some improvement of light yield is observed for a 0.001 ~ 0.005% range of Nb content.

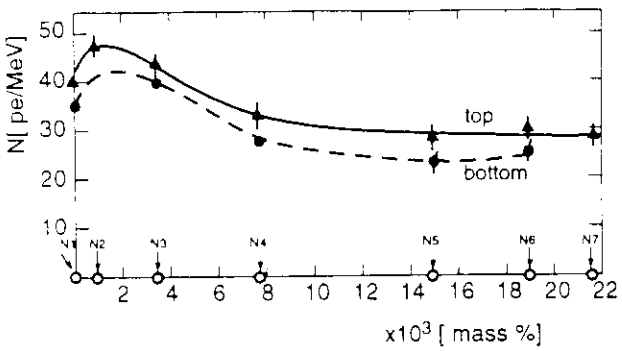

Fig. 4 Light yield of Nb-doped samples ($10 \times 10 \times 10$ mm^3) versus Nb content in the melt during crystal growth.

This can be due to the improved transmission below 450 nm of Nb-doped samples. Nb doping provides a better uniformity of light yield along the crystal.

Table I

180 mm crystal	Top $N_{channel}$	Bottom $N_{channel}$ (near PM window)
PWO undoped	160	190
PWO:Nb (0.0038%)	165	165

Table I gives the relative position (in channels) of the photopeak of the ^{60}Co source for full size elements corresponding to N1 (undoped) and N3 samples, both 180 mm long, when the source is mounted at 1 cm (bottom) and 17 cm (top) from the photomultiplier window. The total light yield of Nb-doped crystal appears to be less than for undoped crystal when the source is near the PM window. A weak absorption band around 420 mm which was not present in the undoped crystal spectra appears and may give a small decrease of light yield. Its origin must be further investigated.

IV. Radiation Damage of PWO:Nb-Crystals

Radiation damage in $PbWO_4$ crystals is caused by charge exchange processes in the Pb^{3+} structure point defects under γ-irradiation. An additional absorption band with a maximum around 620 nm appears for irradiated crystals with an intensity proportionnal to the absorbed dose [5, 9]. The crystal radiation damage near the seed (top part) is 10 times less than what is observed at the bottom part. With compensation of recharging defects, the radiation hardness of $PbWO_4$:Nb crystals is expected to be better.

A. γ-Ray Irradiation

Reference samples N1 (undoped), N3 and N6 (top and bottom) were irradiated by a 500 Rad/s ^{60}Co source up to a 0.5 Mrad absorbed dose. Transmission spectra, γ-ray excited luminescence spectra, scintillation kinetics as well as light yield were measured after irradiation (2–4 h). Transmission measurements are presented in Figs. 5 (a)–(e). $PbWO_4$:Nb crystals are seen as radiation hard even at low Nb content in the crystal.

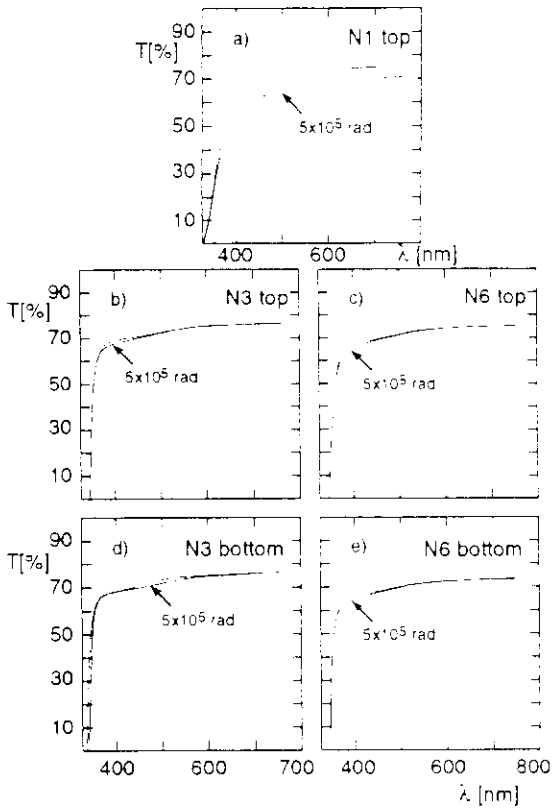

Fig. 5 Changing of optical transmission of undoped (a) and Nb-doped samples extracted from the top (b, c) and the bottom (d, e) of crystals after 5×10^5 rad absorbed dose. Measurements were done 2 h after irradiation.

From these data an estimation of the defects with Pb^{3+} can be made. A compensation already exists for crystal N3 and defect concentration is estimated to be less than 5×10^{17} cm^{-3}. A comparison of crystal characteristics before and after irradiation is given in Table II. A good stability of PWO:Nb crystal to γ-rays irradiation is observed. It indicates a negligible amount of defects recharged by γ-irradiation and structure point defects which could create colour centres in the crystal.

B. Electron Beam Irradiation

The full size PWO:Nb crystal corresponding to reference sample N3 was irradiated along its longer axis with a 500 MeV electron beam at the LIL facility at CERN. The impinging number of electrons corresponded to a 2 Mrad deposit at the maximum of the shower (referred to below as 2 Mrad equivalent). The effect of irradiation on crystal transmission is shown in Fig. 6 for different positions along the crystal from the top side. The homogeneity of the PWO:Nb crystal is indicated by the vicinity of the transparency curves.

Table II

Samples	Light yield phe/MeV before irradiation	Light yield phe/MeV after irradiation	Decay time ns τ_1 τ_2 before irradiation	Decay time ns τ_1 τ_2 after irradiation	λ_{max} nm before/after irradiation
N3 top	44	42	2.7 13.8	2.7 12	495 / 490
N3 bottom	40	48	2.4 11.9	2.4 11	490 / 488
N6 top	30	30	2.2 11.7	2.5 12.3	490 / 490
N6 bottom	25	25	2.3 11.9	2.5 11	488 / 488

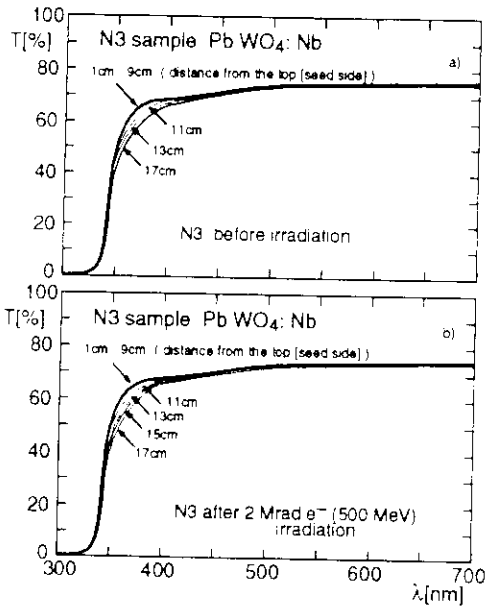

Fig. 6 (a) Initial transmission and (b) transmission after 2 Mrad absorbed dose from e^- beam (500 MeV), measured transversally at different positions from (seed side) along the growth axis.

In Fig. 7 the transmission curves through the 180 mm of the crystal before and after electron irradiaton are displayed. The change of transparency at the emission maximum wavelength (500 nm) is less than 5%.

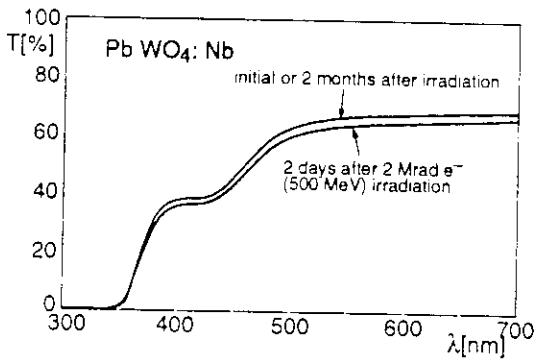

Fig. 7 Changing of longitudinal transmission of PWO:Nb full-size element (180 mm) after 2 Mrad absorbed dose from e^- beam (500 MeV) and self recovery after 2 months delay. T = 300 K.

Two months after irradiation the crystal had fully recovered its original transparency. Finally in Fig. 8 the absorption coefficient induced by irradiation is compared for an undoped crystal from a previous production batch measured in the RD18 collaboration at CERN after 0.076 Mrad irradiation by ^{60}Co γ-rays and for a PWO:Nb crystal after 2 Mrad equivalent irradiation by the LIL electron beam. The doping with Nb further increased the good radiation hardness of normal PWO by decreasing the already small induced absorption coefficient ($\Delta K \sim 2.5$ m^{-1}) by a factor 10 ($\Delta K \sim 0.25$ m^{-1}) for Nb-doped crystal.

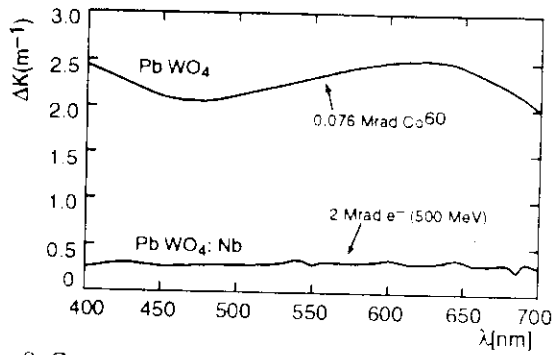

Fig. 8 Comparison of the effect of irradiation on undoped crystals (0.076 Mrad, ^{60}Co, 1.2 MeV) and PWO:Nb (2 Mrad, e^- beam, 500 MeV).

V. Beam Test for Different Crystal Types

A beam test was performed in the X1 beam at CERN for various types of PWO crystal [10]. Energy resolution and temperature dependence of the light yield was measured. The preliminary results of energy resolution with photomultiplier readout for an e^- beam between 10 and 70 GeV are presented in Fig. 9(a) for a matrix of 25 cells ($20 \times 20 \times 180 + 200$ cm^3) of PWO. It fits well the $\sigma E/E = 2.8/\sqrt{E} \oplus 0.45$ formula where 0.3% of the beam momentum spread had been quadratically removed. The same performance is expected for an Nb-doped crystal matrix as can be seen in Fig. 9(b) where 20 GeV/c electron peak hitting a single cell within a 2×2 mm^2 area is shown for an Nb-doped and for an undoped cell. The temperature dependency of the light output of undoped PWO crystal is shown in Fig. 10 and found to be $-2.10 \pm 0.06\%$ °C^{-1} at 17°C. Similar results have been obtained with Nb-doped crystals.

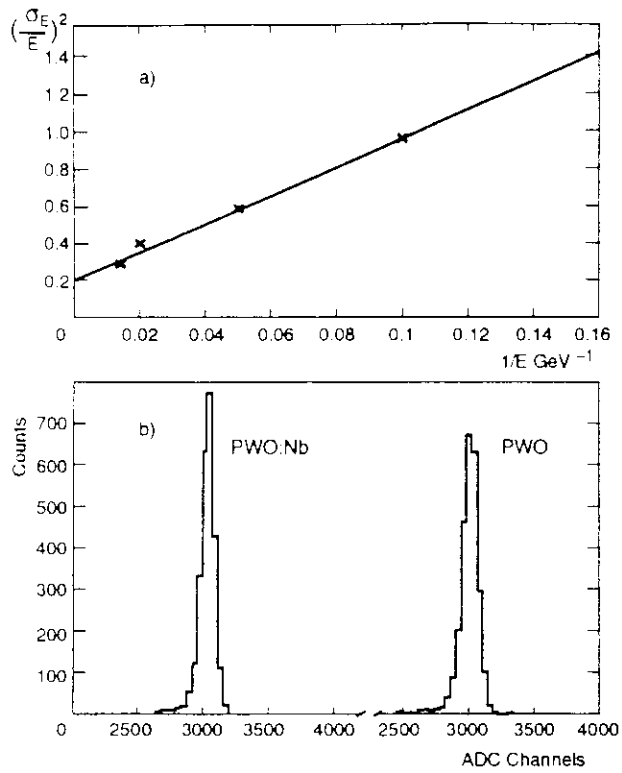

Fig. 9 a) Energy resolution of 5 × 5 Matrix prototype calorimeter of undoped PWO crystal. b) Comparison of 20 GeV electron peak for one undoped and Nb-doped crystal.

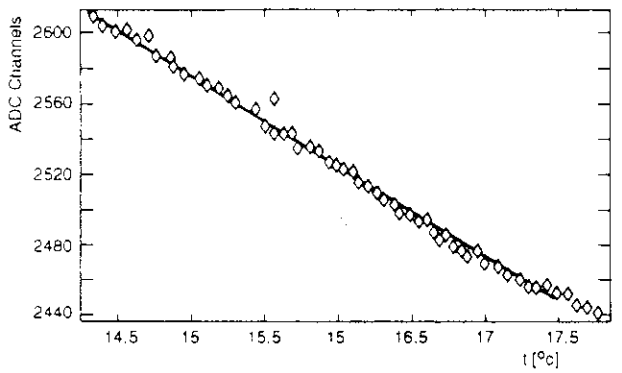

Fig. 10 Light output versus temperature for PWO cell.

VI. CONCLUSION

The tuning of the growing conditions improved the uniformity of the stoichiometric PWO crystal. Crystals grown with Nb doping show improved transmission below 400 nm and, by controlling the occurence of the defect in the crystal based on Pb^{3+} ions, their radiation hardness is increased significantly.

VII. ACKNOWLEDGEMENTS

The authors would like to thank the INTAS foundation which has supported part of this work. They also wish to express their gratitude to Mr J.P. Merlo for his help with access to the LIL irradiation facility, and to Miss E. Auffray and Mr I. Dafinei who quickly provided the transmission measurement on the spectrometer of the RD18 collaboration after LIL irradiation.

VIII. REFERENCES

[1] V.G. Baryshevsky et al., "Single Crystals of Tungsten Compounds as Promising Materials for the Total Absorption Detectors of the e.m. Calorimeters", Nucl. Instrum. Methods Phys. Res., vol. A322, pp. 231–234, 1992.

[2] M. Kobayashi et al., "$PbWO_4$ Scintillator at Room Temperature", in Heavy Scintillators for Scientific and Industrial Applications, Proc. "Cristal [sic] 2000" International Workshop, Chamonix, France, Sept. 1992, Eds. F. De Notaristefani, P. Lecoq and M. Schneegans, Editions Frontières, 1993, p. 375.

[3] V.A. Katchanov et al., presented at the 4th Int. Conf. on Calorimetry in High Energy Physics, La Biodola, Elba, Italy, Sept. 1993.

[4] V.A. Katchanov et al., "Properties and Radiation Hardness of $PbWO_4$ Crystals", in 1993 IEEE Conference Record, Nuclear Science Symposium and Medical Imaging Conference, San Francisco, USA, Oct.–Nov. 1993, p. 146.

[5] O.V. Buyanov et al., "A First Electromagnetic Calorimeter Prototype of $PbWO_4$ Crystals", Nucl. Instrum. Methods Phys. Res., vol. A349, pp. 62–69, 1994.

[6] M.V. Korzhik et al., preprint LAPP-EXP 94–01, submitted to Physica Status Solidi.

[7] S. Inaba et al., "A Beam Test of a Calorimeter Prototype of PWO Crystals at Energies Between 0.5 and 2.5 GeV", KEK Preprint 94–105, submitted to Nucl. Instrum. Methods Phys. Res. A.

[8] M.V. Korzhik et al., "The Scintillation Mechanism in $PbWO_4$ Crystals", presented at MRS'94 Meeting, April 1994, San Francisco, USA.

[9] G. Woody, private communications.

[10] G. Alexeiev et al., to be submitted to Nucl. Instrum. Methods Phys. Res.

PWO EM-calorimeter tests 1994

ALICE/PWO/CMS

X1 beam

- matrix 5×8 with PMT readout with 5 Nb doped crystals;
- matrix 3×3 with EG&G APD;
- matrix 3×3 with PIN diodes 1×1 cm (Hemonets)
- matrix 3×3 with APD 10×10 mm² from Minsk

Energy range 5 to 70 GeV, $\sigma_{beam} \approx 0.3\%$

H4 beam

- matrix 5×5 with PMT readout
- uniformity measurements

Energy range 20 – 150 GeV.

X1 beam

- CMS crystals, matrix 4×4
  - old wrapping
  - new — " — " —

Katchanov V. (Katchano@CERNVM)

[illegible] tests [illegible]

matrix 5x8 PMT readout

AP1911

№ crystals → № ADC → № PMT →	103 L=220 5 3582	20 L=200 10 2872	21 L=180 15 5820	22 L=180 20 33580	2` L=180 25 33895	25 L=200 30 34650	614 L=200 35 7840	613 L=200 40 8729
	205 L=170 4 3400	8 L=180 9 5795	202 L=180 14 5808	24 L=180 19 5815	208 L=18[illegible] 24 5803	610 NB L=200 29 9265	210 L=180 34 3459	615 L=200 39 9150
	204 L=180 3 5782	23 L=200 8 5800	605 L=200 13 5797	602 L=200 18 34699	607 NB L=200 23 3581	612 NB L=200 28 33877	611 NB L=200 33 5593	601 L=200 38 8758
	209 L=190 2 8772	1 L=180 7 5814	201 L=180 12 5789	9 L=180 17 3449	203 L=180 22 3460	606 NB L=200 27 5617	10 L=180 32 2886	603 L=200 37 7341
	101 L=225 1 5780	6 L=180 6 5736	3 L=180 11 5796	104 L=185 16 5781	7 L=180 21 34653	102 L=205 26 5813	604 L=200 31 5613	207 L=180 36 33978

beam

X1 beam tests.

PMT readout

CMS crystals, new wrapping

matrix 4×4

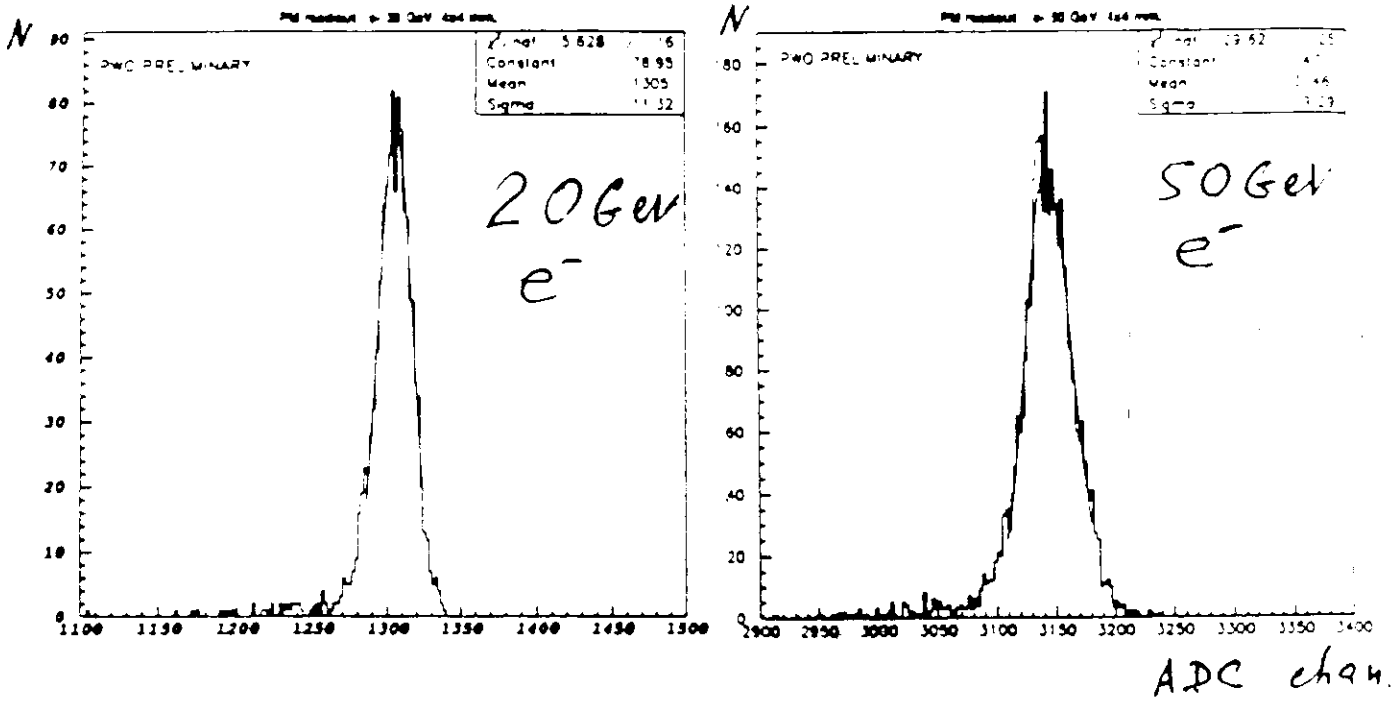

20 GeV: $\sigma/E \approx 0.87\%$ 50 GeV: $\sigma/E \approx 0.61\%$

(without any corrections)

Beam spread is $\sigma \approx 0.3\%$

with a beam correction

20 GeV	50 GeV
$\sigma/E \approx 0.81$	$\sigma/E \approx 0.53$

PWO 5x5 matrix PM1911 readout 6x6 mm. e- beam

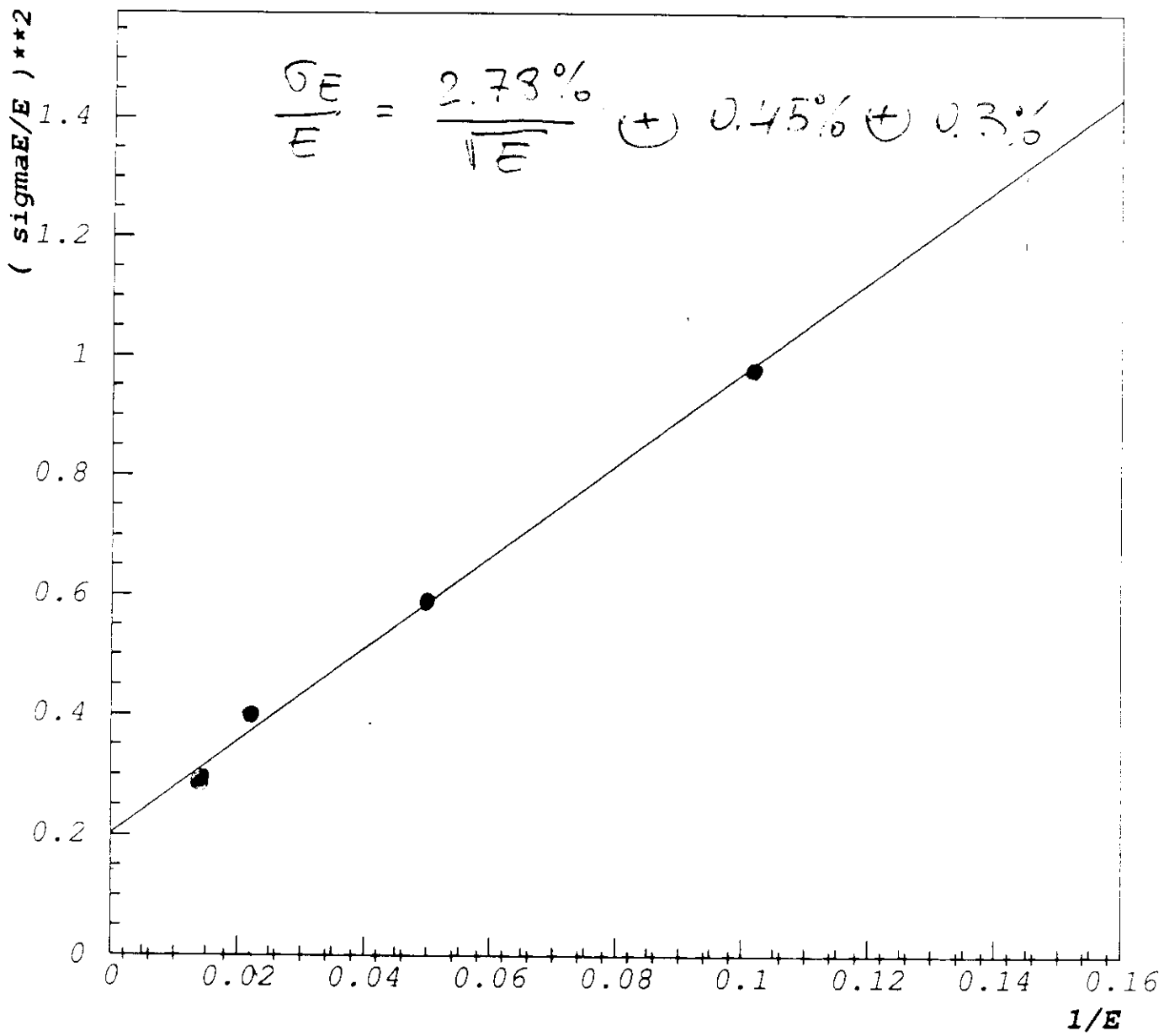

X1 beam tests.

PMT readout

CMS crystals, new wrapping

matrix 4×4

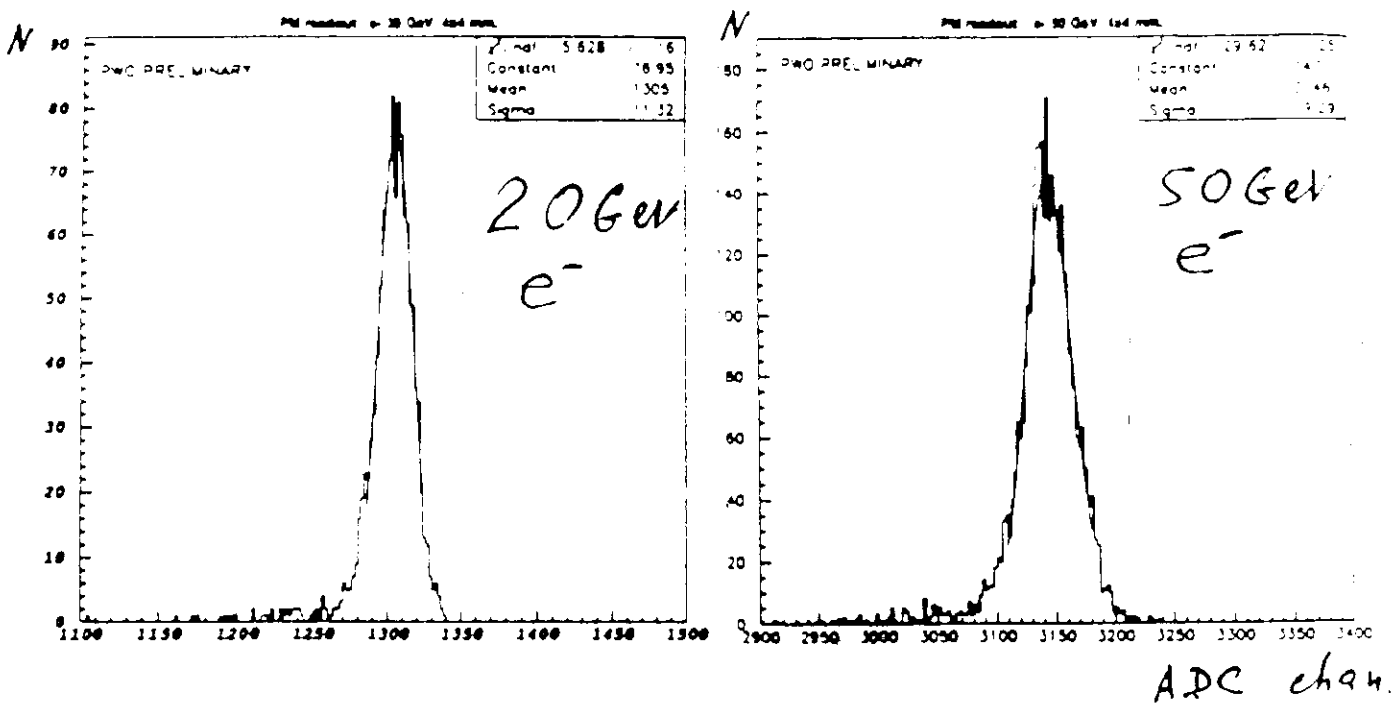

20 Gev: $\sigma/E \approx 0.87\%$ 50 Gev: $\sigma/E \approx 0.61\%$

(without any corrections)

Beam spread is $\sigma \approx 0.3\%$

with a beam correction

20 Gev	50 Gev
$\sigma/E \approx 0.81$	$\sigma/E \approx 0.53$

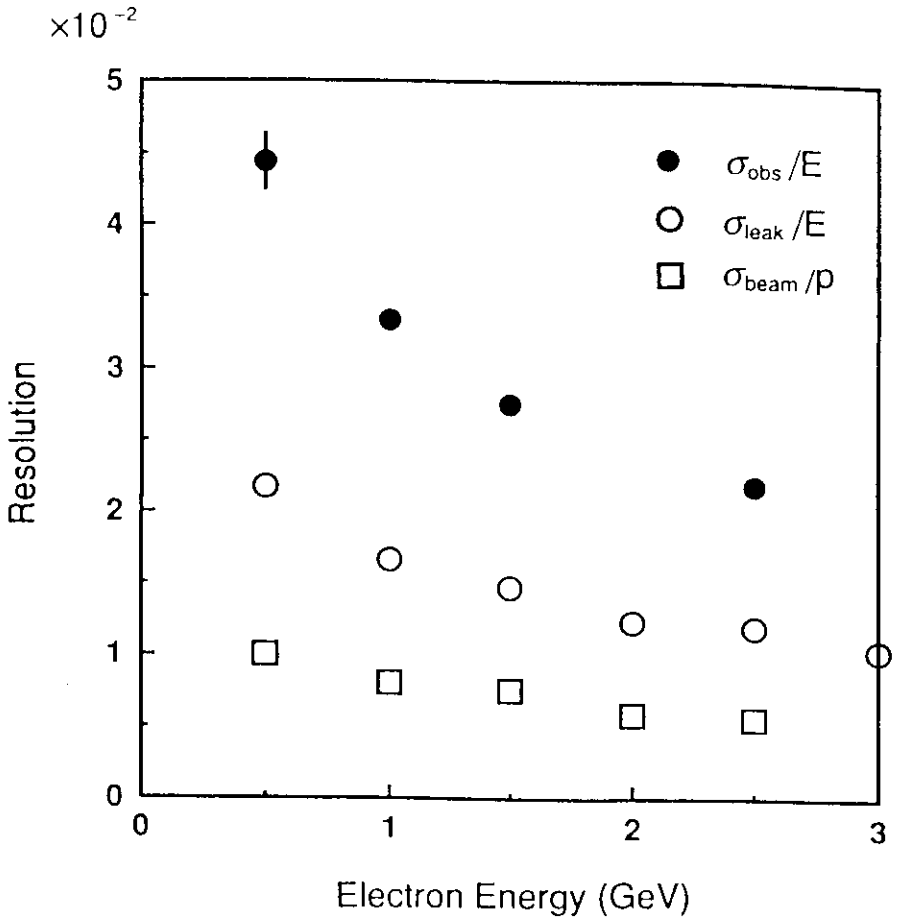
×10 -2
5
4
3
2
1
0
Resolution
σobs /E
σleak /E
σbeam /p
0
1
2
3
Electron Energy (GeV)

Fig. 7.

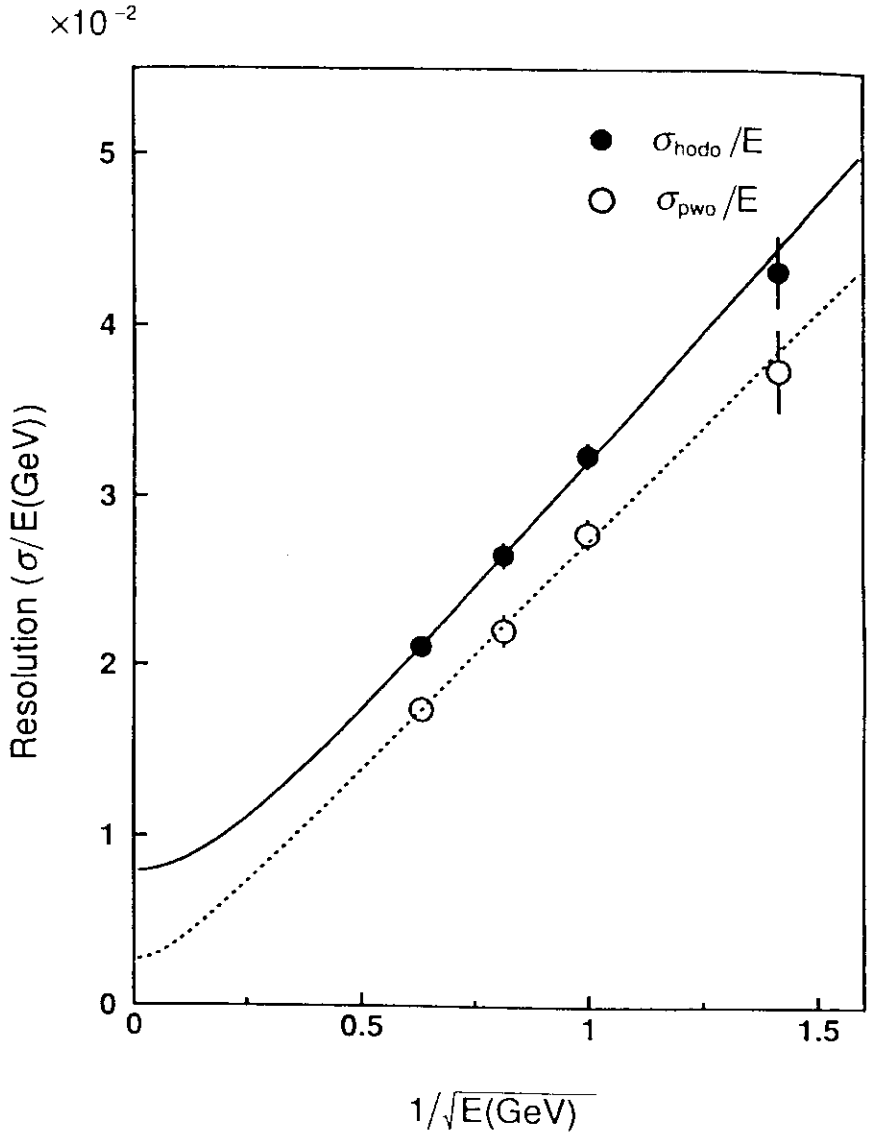
×10 -2
5
4
3
2
1
0
Resolution (σ/E(GeV))
σhodo /E
σpwo /E
0
0.5
1
1.5
1/√E(GeV)

Fig. 8.

ALICE/PWO
matrix 5×6

Preliminary

$PbWO_4$, matrix 3×3
KEK Icsl

K. Takamatsu

PMT readou

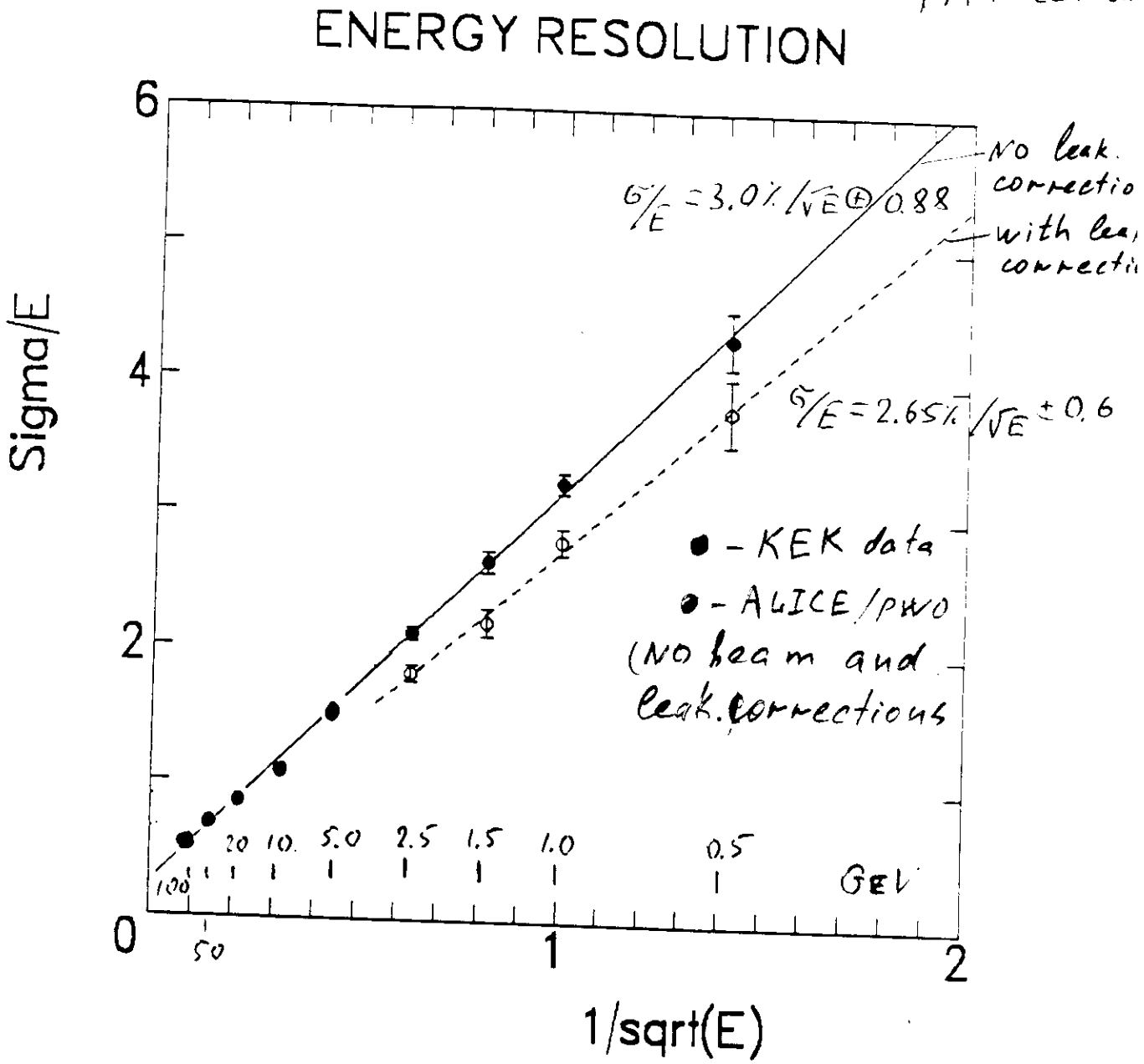

94/08/25 14.1(

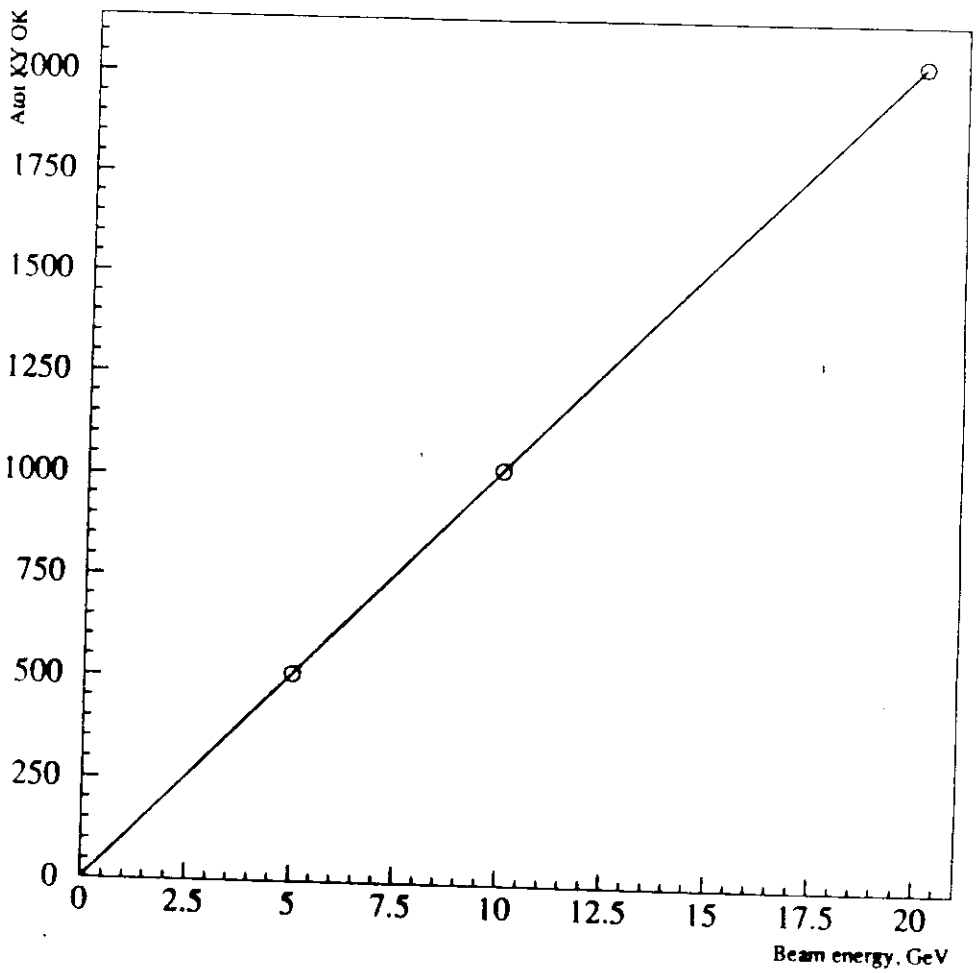

Linearity of PWO EM-calorimeter
23 X_0, from 5 to 20 GeV better than
$\approx 0.1\%$.

Coordinate resolution and lateral profile of EM-shower in $PbWO_4$

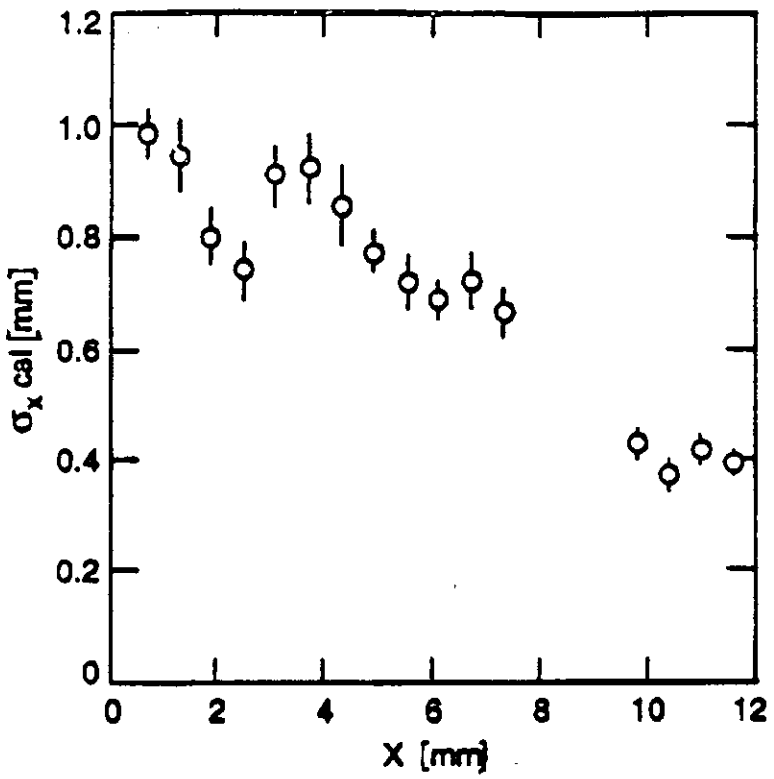

Position resolution as a function of position

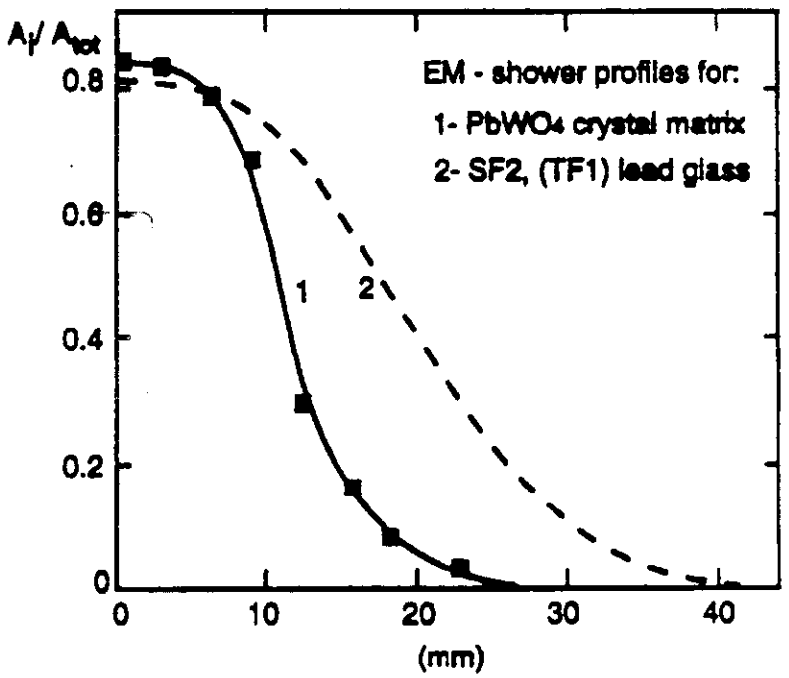

Electromagnetic shower lateral profiles

PIN diode readout

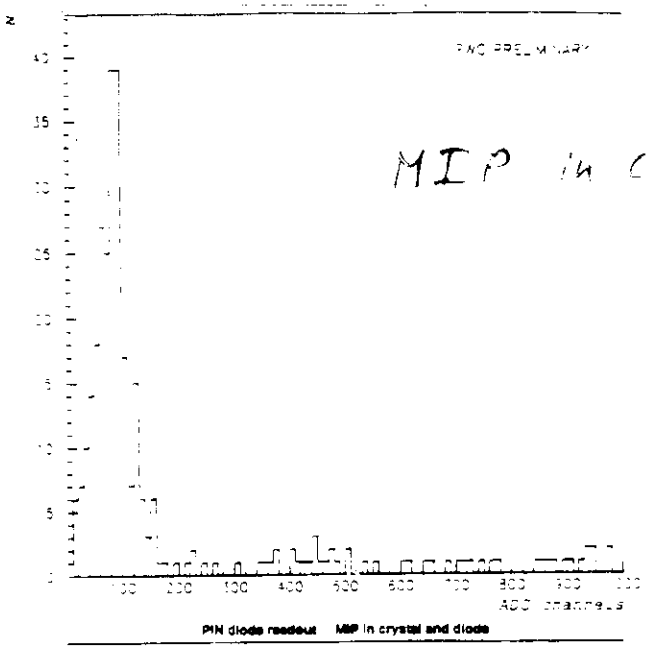

MIP in crystal only, 20 cm

≈ 25 MeV

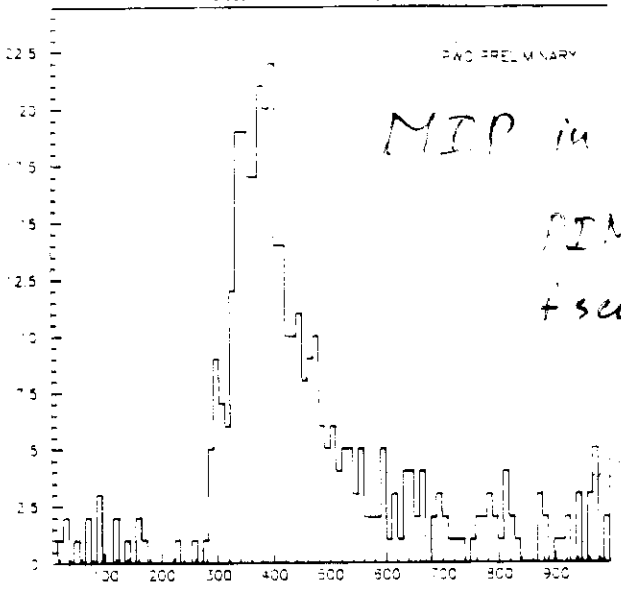

MIP in crystal and diode

PIN diode 300 μm - 15 MeV
+ scint. light

≈ 16 ph. / MeV

Corrections:
- quant. eff. - 0.55
- geom. factor ≈ 4

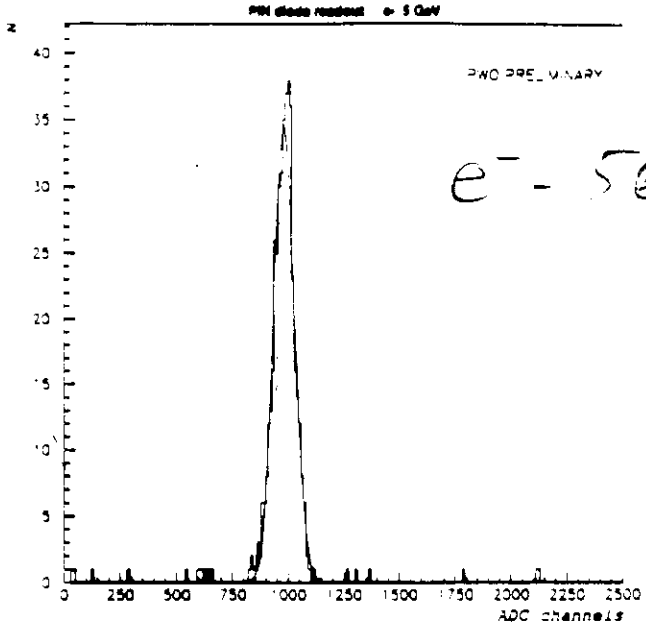

e^- - 5 GeV

L.Y. ≈ 1.5 Ph. / MeV

PWO light yield measurements.

PWO

PIN diode readout

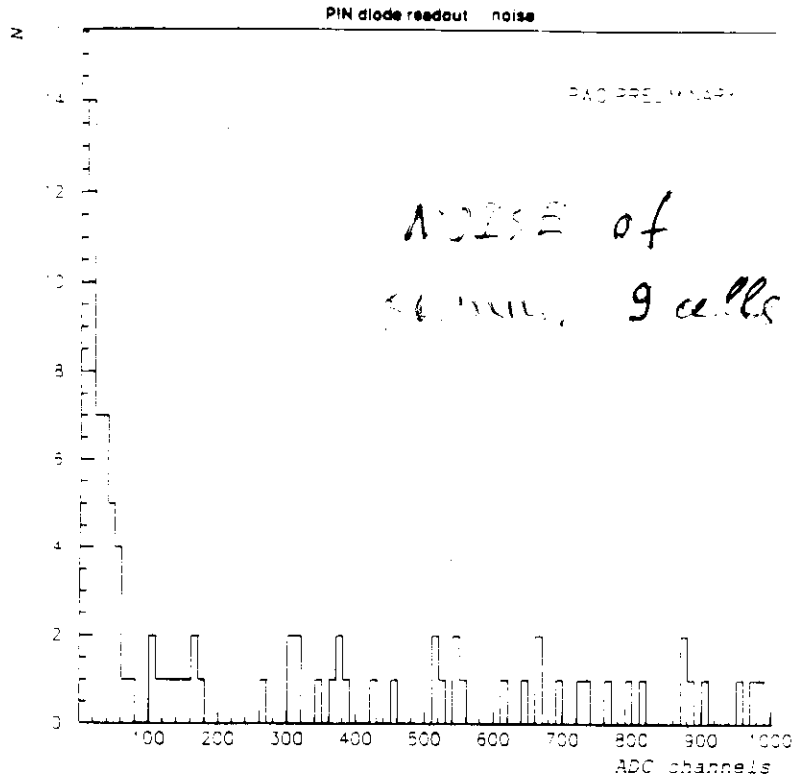

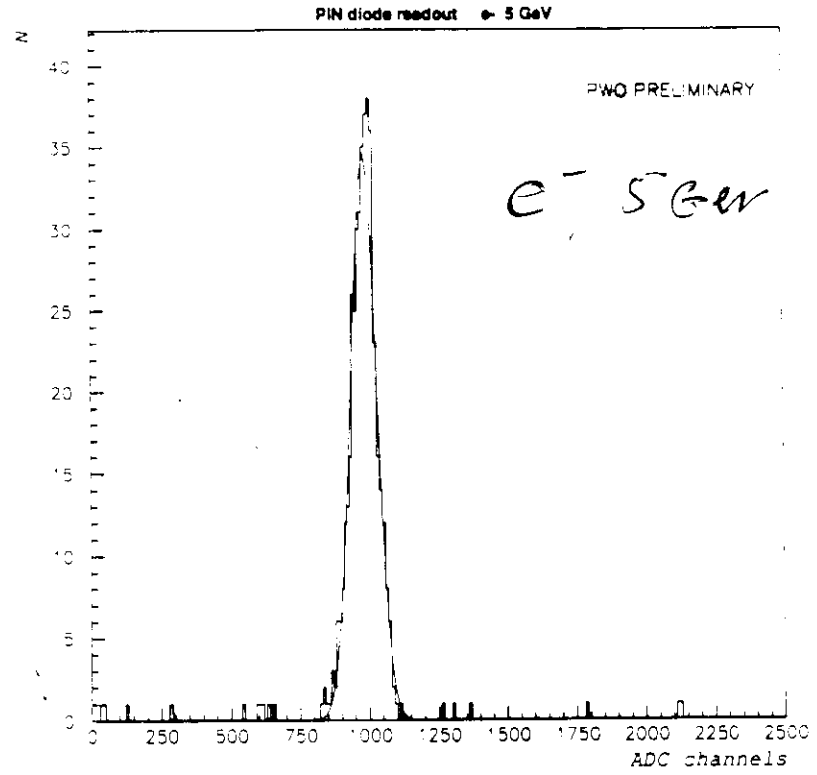

NOISE for PIN diodes readout $\sum_9$

≈ 200 MeV

PWO PM1911 readout. Light yield vs. temperature

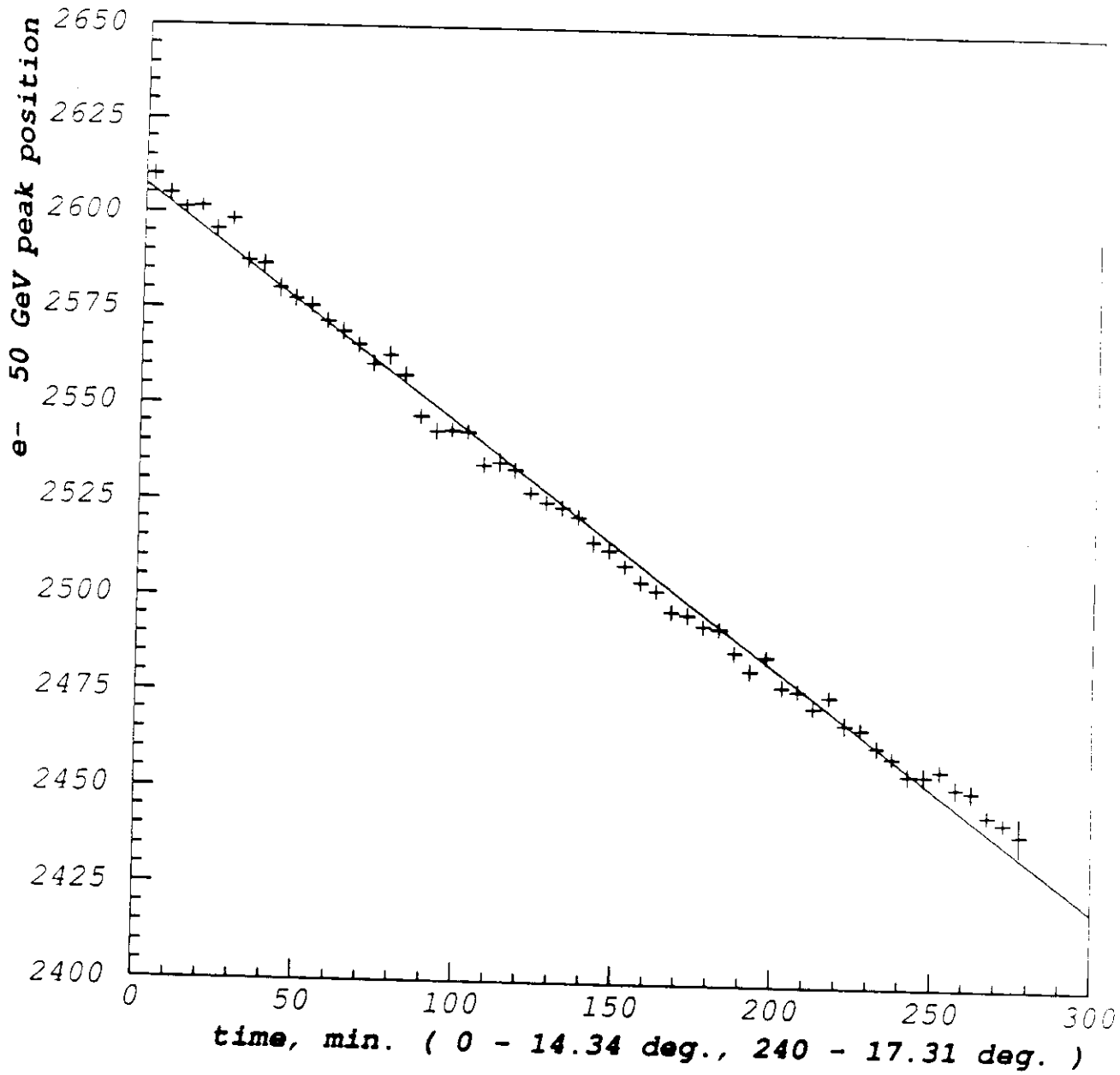

$[(-1.99) \pm 0.01]\,\%/\text{deg.}$

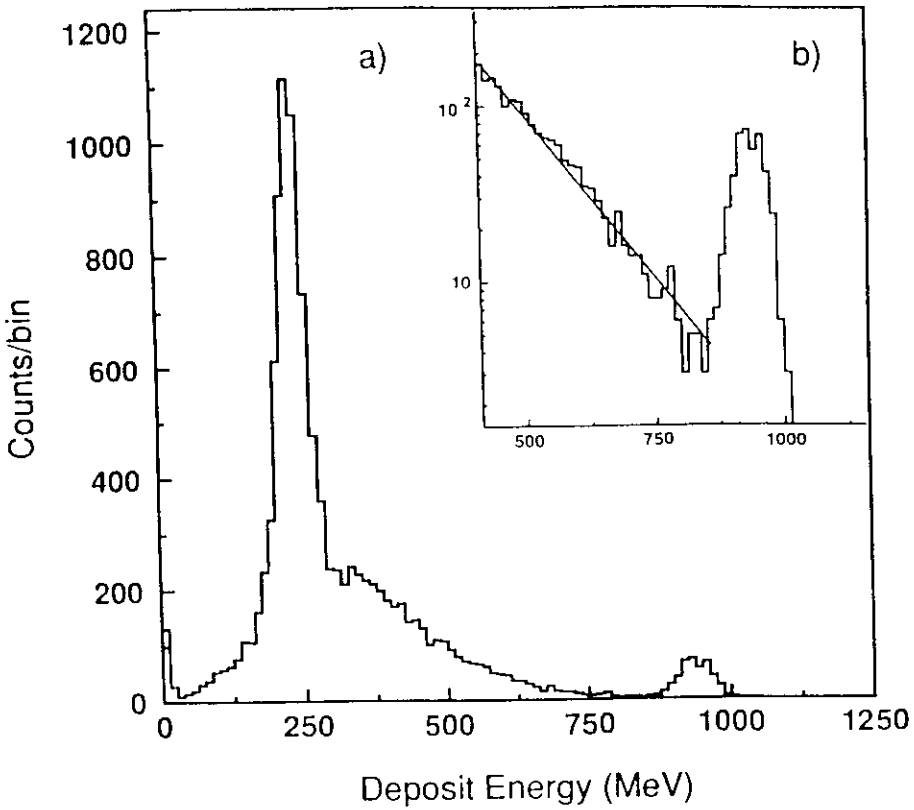
a)
b)
Counts/bin
Deposit Energy (MeV)
0
200
400
600
800
1000
1200
250
500
750
1250
10 2
10
500
750
1000

Fig. 9.

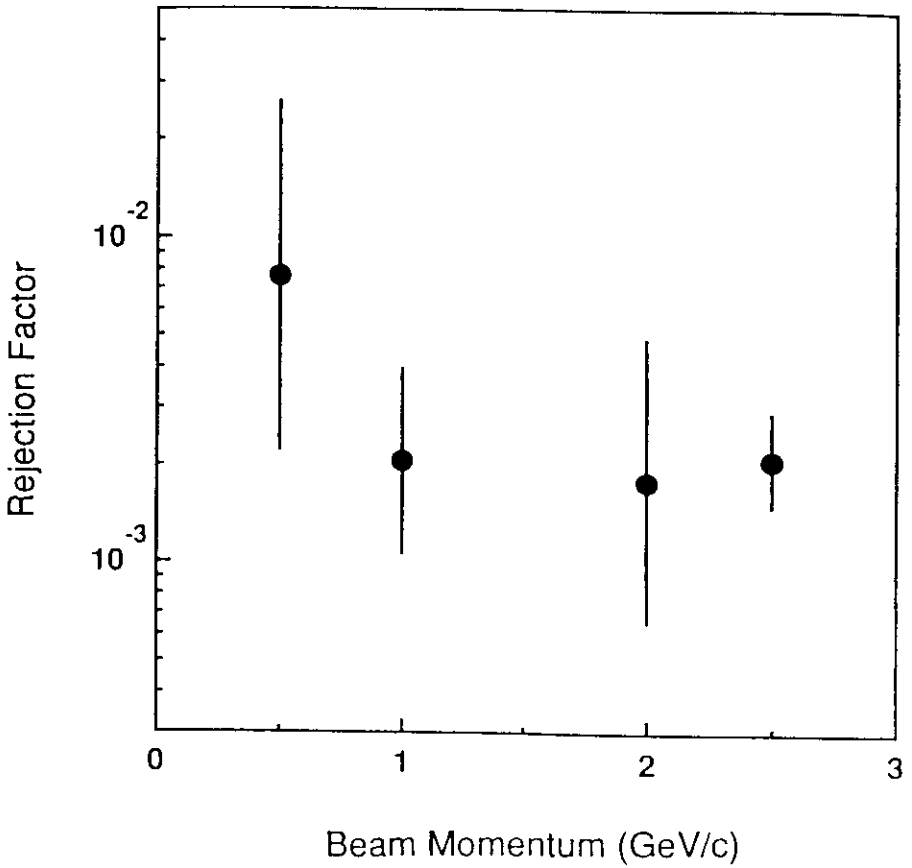
Rejection Factor
Beam Momentum (GeV/c)
10 -2
10 -3
0
1
2
3

Fig. 10.